SHOCK WAVE PRESSURE IN FREE WATER AS A FUNCTION OF EXPLOSIVE COMPOSITION

G. W. Lawrence
Indian Head Division
Naval Surface Warfare Center
Research and Technology Department
Indian Head, MD 20640

Free field pressure measurements were performed underwater on shock waves produced from detonated charges. The properties of the ingredients in an underwater explosive control the characteristics of the shock wave. The data can be analyzed in terms of early vs. late time release of energy. For a given peak pressure the peak width, the energy, and impulse increase with more late time energy release.

INTRODUCTION

The properties of the various ingredients in an underwater explosive control the characteristics of the shock wave. After the explosive detonates, a gas bubble with high interior pressure is formed in the water. This pressure expands the bubble rapidly. Consequently, the pressure generated in the water by the rapidly expanding gas bubble creates and supports the shock wave. If all of the energy is released during the detonation process as for ideal ingredients, the physics of the bubble expansion controls the energy utilization and the characteristics of the shock wave. If there is post-detonation energy release as for non-ideal materials the kinetics of these late time reactions modify the energy available to the gas bubble expansion. This late time energy is released by oxidation-reduction reactions initiated by the detonation. The kinetics of these reactions determines how fast additional energy is released to support the bubble expansion before the shock wave becomes detached from the bubble. The kinds of ingredients, their ratio, and their particle size modify these kinetically controlled reactions. The test results from eight compositions are analyzed to explain how the various properties of the ingredients modify the shock wave characteristics.

EXPERIMENTAL METHOD

Charge Preparation

All PBX charges (See Table 1.) were cast from a 19-liter vertical mixer, using standard mixing procedures into PVC cylinders (20.32 cm X 20.32 cm). The charges had a conical pentolite charge affixed to the top of the cylinder and then were fitted with a detonator. Pentolite charges were pellet loaded.

Table 1 shows the explosive ingredients and particle diameter of the solids for the compositions under consideration. Metal is typically present at 25 – 30%, oxidizer at 30 – 50%, and explosive (HE) at 0 – 15%.

Table 1: Explosive Ingredients and Nominal Particle Diameter of Solids

Composition	Al	Oxidizer	Oxidizer2	HE	Binder
1	26 μ	200 μ AP			NE
2	18 μ	200 μ AP		RDX (1/5)	PUH
3	10 μ	200 μ AP		RDX 5	PUNA
4	12 μ	200 μ AP		HMX 3	PUNE
5	12 μ	200 μ AP	fine fe_2o_3	HMX 3	PUNE
6	12 μ	200 μ AP	fine fe_2o_3/al_2o_3	HMX 3	PUNE
7	12 μ/18 μ	200 μ AP	90 μ AP	HMX 3	PUNE
8		PETN		TNT	

NE = nitrate ester, PUH = polyurethane hydrocarbon, PUNA = polyurethane nitroaliphatic hydrocarbon, PUNE = polyurethane nitrate ester

Data Collection

The charges were detonated in a large body of water at a depth of 19.81 m. A pressure gage (Tourmaline) array at standoffs of 1.22, 2.44, 4.88, and 9.75 m was deployed at the same depth and was used to measure the shock wave profile of the 3-dimensional pressure decay. The gage records were collected digitally and stored for analysis.

Data Reduction

The shock wave[1] is characterized by peak pressure (P_{max} = P at t = 0, where peak pressure rise starts), peak width (θ = t when P = P_0/e, decay constant), energy ($1/\rho c \int P^2 dt$) (ρ=density & c=sound speed of water), and impulse ($\int P\, dt$) as a function of distance and time for each gage. All integrations are performed to 1.3 msec from t = 0 for each gage. In general the pressure (P) variation with time (t) is fit to an analytical expression, a decaying exponential plus a constant (See Eq.1), by minimizing the difference between the experimental and fit impulse with time.

$$P = P_0 e^{-t/\theta} + C_0 \qquad \text{Eq. 1}$$

While the observation time is of the

order of 25 msecs, the fit to Eq. 1 for many materials for all gage ranges is limited to 1.3 msec for these size charges by the decay of the pressure at long times (See Graph 1.) The fitting procedure smoothes any irregularities in the data and covers a major portion of the significant data. Generally, the small rise in data in the middle is not fit. This small error is compensated by the flatness of the fitted curve, which over calculates the decay of the data at longer time.

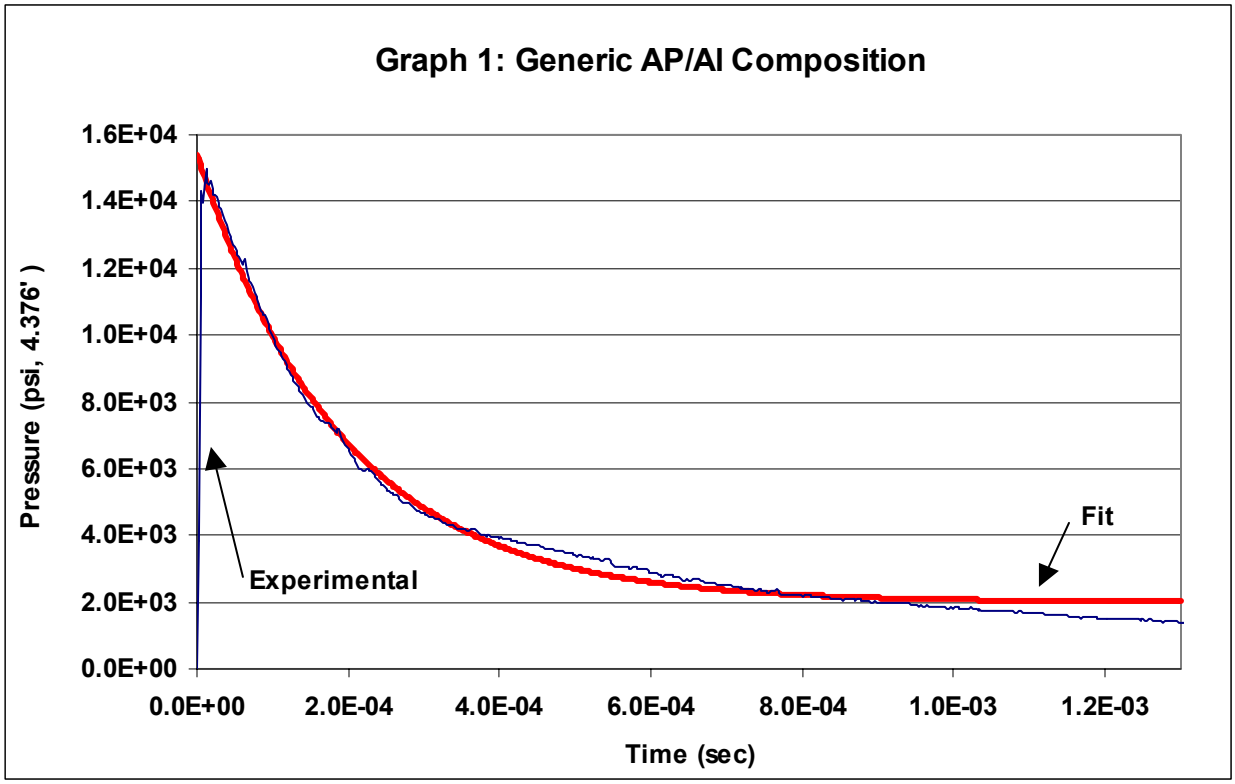

From the fit expression the characteristics of the wave are calculated for the eight compositions. These characteristics are then fit to similitude parameters[1], K and α (See Eq. 2), as function of weight (W) and range (R).

$$Characteristic = K(\frac{W^{1/3}}{R})^{\alpha} \qquad \text{Eq. 2}$$

where *Characteristic* is divided by $W^{(1/3)}$ for decay constant, energy and impulse.

The similitude equations are then used to correct for booster contributions, to normalize the characteristics of different explosives, and to compare them by calculating an equivalent mass[1] relative to a standard averaged over a reduced range of 2.5 m.

Calculations

1-D hydrocode calculations are done using CTH[2-3] for a sphere of explosive. A generic AP/Al composition is modeled using a JWL equation of state with kinetic dependence for late

time energy release.[4] Graph 2 shows the results for a charge of similar mass at a similar distance to the experimental charges. The rise in data in the middle is more accentuated in the calculated pressure trace than the experimental one (Graph 1). The small peaks in the middle of the curve are caused by shock wave reflections inside the bubble passing into the water at a slightly later time.

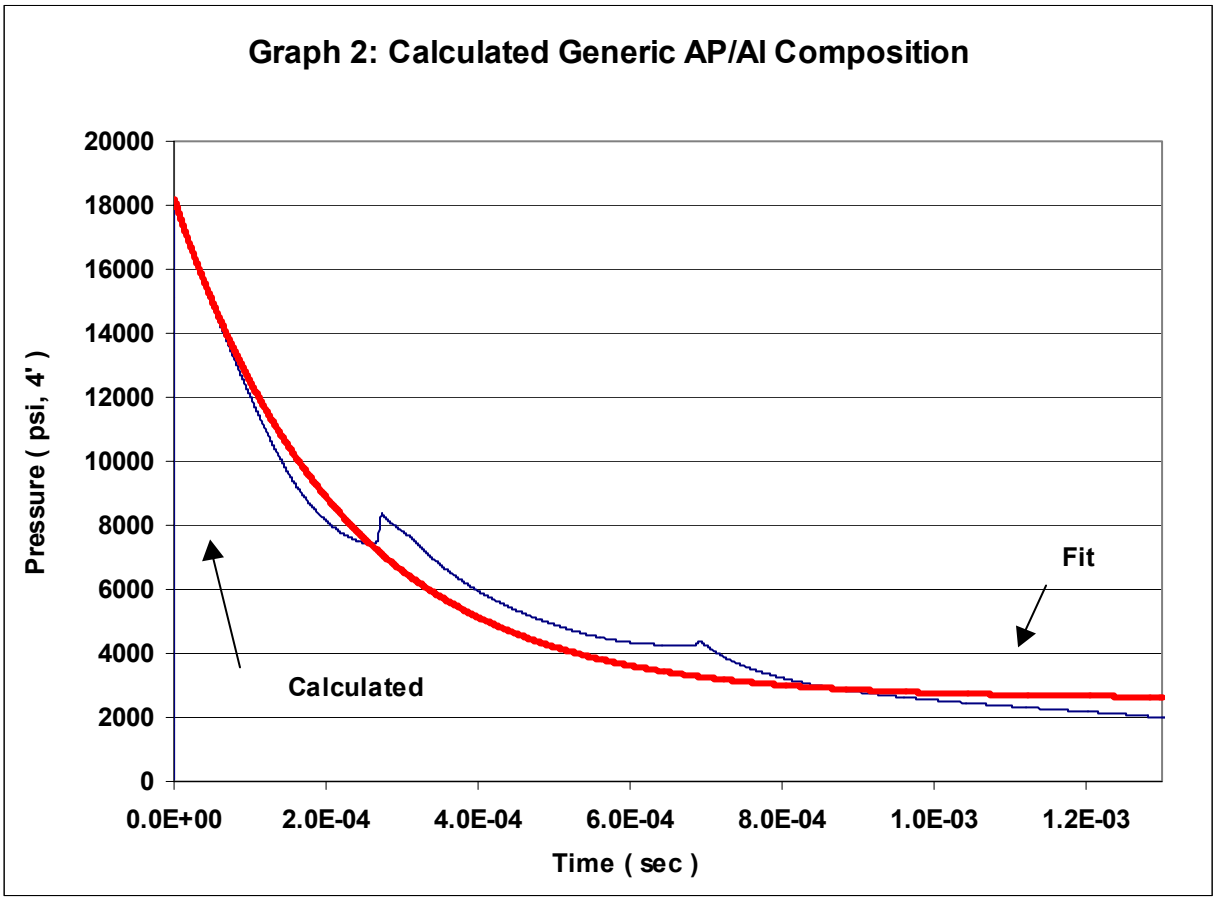

The equivalent mass results from 4 small calculations for a 2-cm sphere are shown in Table 3. The rate constant for energy release varies from 25 to 85 with 65 taken as standard. The calculated data are treated in the same manner as experimental data. Since these CTH calculations are done on a much smaller scale than the experimental tests the pressure traces cannot be directly compared. Since the similitude constants are derived for materials having late time energy release they don't apply strictly either.

RESULTS

The reactivity of many different fuel-oxidizer combinations can be observed in this way.

Table 2 shows the relative experimental results on equivalent mass basis for the eight compositions.

Table 2: Relative Pressure Trace Characteristics

Composition	Theta	Pmax	Energy*	Impulse*
1	1.000	1.000	1.000	1.000
2	1.579	0.818	0.935	0.974
3	1.096	1.161	1.131	1.067
4	1.025	0.973	0.977	0.969
5	0.973	0.942	0.947	0.943
6	0.957	0.925	0.937	0.935
7	0.863	1.001	0.977	0.966
8	0.200	0.996	0.793	0.848

* All gages integrated to constant time

Table 3 shows the calculated results on an equivalent mass basis of varying the time dependence of the late time energy release while keeping the early time parameters constant for a generic AP/Al composition.

Table 3: Calculated Relative Pressure Trace Characteristics

Kinetic Constant	Theta	Pmax	Energy*	Impulse*
65	1.000	1.000	1.000	1.000
25	0.890	0.970	0.896	0.842
45	0.922	0.970	0.941	0.922
85	1.106	0.970	1.0387	1.067

* All gages integrated to constant time.

As the kinetic constant is increased, peak pressure stays nearly constant but the other characteristics increase.

DISCUSSION

The properties of the ingredients in an underwater explosive modify the characteristics of the shock wave. For Compositions 1 – 7 the ingredients and ingredient ratios are chosen to optimize the energy characteristic. The more ideal composition 8 gives a shorter decay constant

and less energy than the more non-ideal materials containing AP as expected, but the peak pressure has decayed significantly at this range and is similar to the peak pressures of the more non-ideal materials containing AP. For this result to be true the aluminum and AP must be participating in the reactions in this time frame. Considering that the amount of HE in composition 2 is greater than for any other composition, the decay constant is relatively long and the Pmax is relatively small. The result is probably indicative of a smaller amount of gas in the reaction products than for the other materials. The hydrocarbon binder is probably more unreactive in this time frame than the more energetic binders. Composition 3 has the smallest amount of HE of any HE containing composition, but has an energetic binder giving a higher peak pressure. The finer aluminum may be reacting a little more completely to give a little more energy. The ingredients in Compositions 4 – 6 are adjusted to achieve nearly Composition 1 performance while containing HE. Although fine fe_2o_3 and al_2o_3 could modify the AP decomposition rate, they appear to have no affect in the presence of the HE and act as inert material to lower the overall performance characteristics slightly. Fine AP keeps the peak pressure up and reduces the time constant of Composition 7.

Table 3 demonstrates the trends to be expected if late time energy release were the sole factor in the experimental results. By applying these calculated trends to the observed data additional trends in the observed data can be confirmed. Composition 4, having similar characteristics to Composition 1, appears to have balanced the early and late time reactions with HMX replacing much of the NE. Compositions 5 – 6 have kept the balance, but have lost characteristic performance slightly because of the addition of inert material (fe_2o_3 and al_2o_3). The fe_2o_3 and al_2o_3 as potential catalysts were unable to alter the balance between early and late time characteristics. In Composition 7 the 90 μ AP increases the importance of early time reactions by decreasing theta without any change to late time reactions with the aluminum. The finer aluminum in Composition 3 appears to increase the late time reactions for all characteristics, but since Pmax is larger, the increase in energy is probably not caused by late time energy release, but by the increased Pmax. The increased theta and decreased Pmax for Composition 2 are caused by a change to early reactions rather than an increase in late time energy release since the other characteristics are not also increased.

SUMMARY AND CONCLUSIONS

The characteristics of the non-ideal materials lie in a relatively narrow range. For this set of compositions the kind of ingredient and the particle size have small but discernable effects on the shock wave characteristics. The oxidizer HE combination does not offset the inert binder effects. The energetic binder by increasing Pmax yields more energy and impulse. While the smaller aluminum particle size can increase the shock wave characteristics, this effect can be offset by having a larger amount of HE present. Finer particle size AP increases the early energy release, but this effect on presumed earlier availability of oxidizer gases does not lead to more late time energy release. If a wider range of particle sizes were formulated, would the characteristics show more variation? If more of the aluminum were to react in the late time regime, would the late time energy release be increased or would it be offset by a decrease in the amount of gas in the bubble?

REFERENCES

1. Robert H. Cole, “Underwater Explosions”, Princeton University Press, Princeton, 1948.
2. J.M. McGlaun, S.L. Thompson, L.N. Kmetyk, and M.G. Elrick, "CTH: A Three-Dimensional Shock Wave Physics Code," Int. J. Impact Engng. 10, 351-360 (1990).
3. W. W. Erickson, “CTH-Reference Manual: JWL-TD”, Sandia National Laboratories MS-0836, April 2000.
4. P. J. Miller and R. H. Guirguis, Experimental Study and Model Calculations of Metal Combustion in AP/Al Explosives”, in Structure and Properties of Energetic Materials, MRS Publication, vol. 296, page 299, 1994.

Address:

Indian Head Division
Naval Surface Warfare Center
101 Strauss Ave.
Indian Head, MD 20640
Attn: G. W. Lawrence, Code 910H, Bldg 490
LawrenceGW@ih.navy.mil
301-744-2589